Analog Realization of the Quantum Derivative Operator

F. Acar Savaci
Electronics and Communication Engineering
Izmir Institute of Technology
Izmir, Turkey
acarsavaci@iyte.edu.tr

R. Ugras Erdogan
Faculty of Medicine, Biophysics Department
Dokuz Eylul University
Izmir, Turkey
ugras.erdogan@deu.edu.tr

***Abstract*—In this paper, quantum derivative operator which is basic to quantum calculus has been implemented as an analog circuit. The proposed circuit realization and the simulations have been also compared with that of the quantum derivative operator implemented in Mathematica.**

Keywords—Quantum Calculus; q-number; q-oscillator; analog q-differentiator; analog q-computing.

INTRODUCTION

Quantum calculus (q-calculus) can be regarded as an ordinary calculus without limit operator [1]. L. Euler initiated the q-calculus in the track of Newton's infinite series and developed Euler's Identities for q-exponential functions. The development of q-binomial formula by Gauss, and the development of Heine's formula for q-hypergeometric series resulted in the advancement of q-calculus in the 19th century [2], [3]. At the beginning of the 20th century, Jackson as one of the most leading mathematicians in this field developed Euler-Jackson q-difference operator and q-integral [4].

Due to the recent advances in this field, q-calculus has found application areas in statistical mechanics; on the self-similar systems and fractals [5], [6]; dynamic equations on time scales (q-analogue of differential equations) [7]; q-analogue of harmonic oscillator [8]; q-analogue of shock soliton solution [9]; on the generalizations of quantum mechanics such as the motion governed by q-partial differential equations that describes diffusion on a topologically uniform lattice [10].

In this study, the main motivation to implement the q-derivative circuit is that it would be the basic tool to achieve analog q-computing, and hence, to solve the dynamic equations on time scales [7] could be possible with its corresponding analog realization.

This paper is organized as follow: In section II, the mathematical definitions of q-derivative and q-number with simple examples and Mathematica implementations of the q-derivative operator have been given to clarify this basic operator of q-calculus. In section III, our proposed circuit realizing the q-derivative operator is presented with the SPICE results. In section IV, the hardware realization of our proposed q-derivative circuit and its oscilloscope traces are presented in comparison to the simulation results. In section V, the conclusion and the future plans are presented.

MATHEMATICAL BACKGROUND

The q-derivative of the function $f(x)$ is defined in [1], [2] as

$$D_q f(x) := \frac{d_q f(x)}{d_q x} \tag{1}$$

where the q-differential of x is defined as

$$d_q x := (q-1)x \tag{2}$$

and the q-differential of the function $f(x)$ is be defined as

$$d_q f(x) := f(qx) - f(x) \tag{3}$$

and hence $D_q f(x)$ can be expressed as

$$D_q f(x) := \frac{f(qx) - f(x)}{(q-1)x} \ . \tag{4}$$

The q-derivative in (4) measures the rate of change of the function with respect to scaling of its argument by a q factor, while as the ordinary derivative is the rate of change of the function in terms of the incremental translation in its argument.

The following simple examples are introduced to clarify the q-derivative concept and the q-number before the proposal of our circuit realization of q-differentiator.

Example 1. The q-derivative of a function, $f(x) = x^n$, is given as

$$D_q x^n = \frac{(qx)^n - x^n}{(q-1)x} = \frac{q^n - 1}{q-1} x^{n-1} = [n]_q \, x^{n-1} \tag{5}$$

where x is a real number and the q-number of (q-analogue of) a positive integer n with the base q is defined as

$$[n]_q := \frac{q^n - 1}{q-1} = q^{n-1} + \ldots + 1 \ , n \in Z^+, \ q \in R \setminus \{1\} \ . \tag{6}$$

978-1-5386-3974-0/17/$31.00 ©2017 IEEE

In the limiting case, as the base q approaches *1*, $[n]_q$ approaches the ordinary positive integer n and $D_q f(x)$ approaches the ordinary differentiation as

$$\lim_{q\to 1}[n]_q = n\ ,\ n\in Z^+ \tag{7}$$

$$\lim_{q\to 1} D_q\, f(x) = \frac{d\, f(x)}{d\, x}\ ,\ x\in R \tag{8}$$

Example 2: Scalar dynamic equations on time scales [7]. The solutions of certain scalar dynamic equations on time scales are exponential functions on the particular time scale.

$$D_q\, f(x) = \frac{f(qx)-f(x)}{(q-1)x} \ = \ a\, f(x) \tag{9}$$

where the solution of (9) is $f(x) = C\, e^{ax}$ on the particular time scale for a constant C.

Example 3: Visualization of the q-derivative of a sinusoidal function. Mathematica plots of $D_q f(x)$ for $q = 2$ and $q = 0.5$ where, $f(x) = \sin(x)$, are shown in Fig. 1, and Fig. 2, respectively.

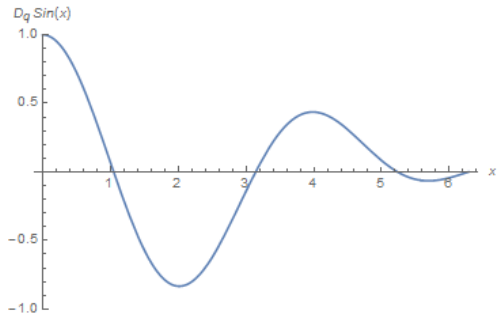

Fig. 1. q-derivative of $f(x) = \sin(x)$ in $[0, 2\pi]$ for $q = 2$.

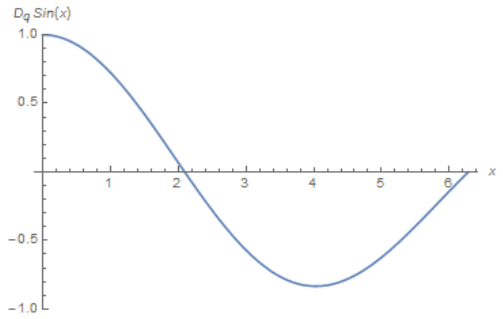

Fig. 2. q-derivative of $f(x) = \sin(x)$ in $[0, 2\pi]$ for $q = 0.5$.

Example 4: q-Harmonic Oscillator [8]. The q-deformed classical harmonic oscillator is

$$D_q^2\, f(x) + \omega^2 f(x) = 0 \tag{10}$$

where the solution of (10) is given as

$$f(x) = A(x)\cos_q(\omega x) + B(x)\sin_q(\omega x)\,. \tag{11}$$

$A(x)$ and $B(x)$ are q-periodic functions and can be arbitrary constants. $\cos_q(\omega x)$ and $\sin_q(\omega x)$ are q-trigonometric cosine and sine functions respectively.

Q-Derivative Operator Circuit Simulation

In this section, the q-derivative circuit is simulated and implemented for the sinusoidal input, $f(x) = \sin(x)$, and the scaling parameter $q = 0.5$. The scaling parameter q can be controlled by setting the necessary values for the capacitors or the multiturn rheostats. Therefore, the circuit has been realized for a general q parameter. For the SPICE simulation, National Instruments Multisim 14.0 is used. The circuit is fed by a symmetric power supply with V_p=*12*V, V_n = *–12*V. The SPICE simulation consists of four subcircuits with the following tasks namely the synthesis of the triangle wave signals, the difference of the triangle wave signals, the sinusoidal wave signals and the q-derivative signal for the sinusoidal input.

A. Synthesis of the Triangle Wave Signals

The triangle wave signals [1] $\mathrm{tri}(x)$ and $\mathrm{tri}(qx)$ are required to synthesize the sinusoidal waveforms $f(x)$ and $f(qx)$ respectively. The signal $\mathrm{tri}(qx)$ has a frequency q times that of the signal $\mathrm{tri}(x)$. The signal $\mathrm{tri}(x)$ corresponds to the independent variable x of $f(x)$, and the signal $q\mathrm{tri}(x)$ having an amplitude q times that of the signal $\mathrm{tri}(x)$ corresponds to the independent variable qx of $f(qx)$ respectively, as shown in (4). Moreover, the signals $\mathrm{tri}(x)$ and $q\mathrm{tri}(x)$ are used to synthesize the difference signal $q\mathrm{tri}(x)$–$\mathrm{tri}(x)$ which represents the difference qx–x due to the scale change in the independent variable x shown in (4). Due to the fact that $f(x)$ and $f(qx)$ have been synthesized using the signals $\mathrm{tri}(x)$ and $\mathrm{tri}(qx)$ respectively, the analog q-derivative signal has been observed over one period.

This subcircuit consists of two triangle wave oscillators with frequencies $f_1 = 2$ Hz and $f_2 = qf_1 = 1$ Hz to synthesize the triangular wave signals $\mathrm{tri}(x)$ and $\mathrm{tri}(qx)$ respectively. For the simulation purposes $f_1 = 1$ kHz and $f_2 = qf_1 = 0.5$ kHz are chosen respectively to observe the waveforms in a shorter time frame. The operation frequency should be in the bandwidth of the circuit elements. The operation characteristics of the triangle wave oscillator can be found in [11] and [12]. The oscillator with *1* kHz oscillation frequency to synthesize triangle wave signal $\mathrm{tri}(x)$ is shown on the top left and the circuit needed to synthesize the signal $q\mathrm{tri}(x)$ from the signal $\mathrm{tri}(x)$ is shown on the bottom of Fig. 3, respectively. The oscillator that has been used to synthesize the signal $\mathrm{tri}(qx)$ has the same circuit topology with that of the oscillator synthesizing $\mathrm{tri}(x)$ with the only difference being $C_1 = 200$ nF for the signal $\mathrm{tri}(qx)$. Therefore, it is not shown in Fig. 3 due to the page limitations. The oscillator frequency can be found as,

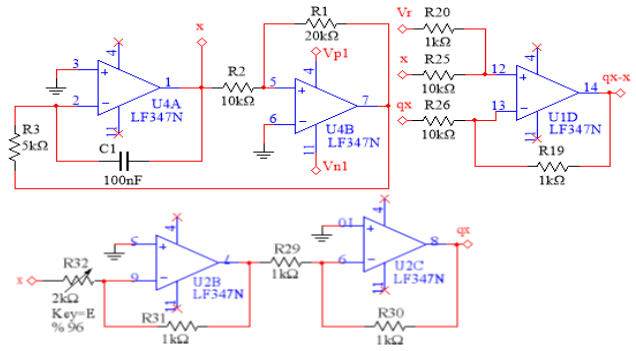

Fig. 3. The synthesis of the signals tri(x), qtri(x) and qtri(x)—tri(x).

$$f_{osc} = \frac{R_1 / R_2}{4 R_3 C_1}. \tag{12}$$

In the circuit implemented to synthesize the signal tri(qx), the multiturn rheostats and the capacitor controlling the oscillation frequency f_{osc} can be tuned to obtain any scaling parameter q. Hence, the frequency scaling control over the signal tri(qx) which is used to synthesize f(qx) has been established. Hence, the frequency scaling parameter q of f(qx) in (4) can be controlled as intended. The amplitude scaling parameter q of qx in the denominator of (4) can be tuned for the intended value via the multiturn rheostat R_{32} in Fig. 3.

B. *Synthesis of the Difference of the Triangle Wave Signals*

The differential amplifier topology used to synthesize the signal $q$tri(x)–tri(x) to be used as the denominator of the q-derivative operator is given on the top right of Fig. 3. The offset voltage V_r is used to prevent the divergence of the simulation and the saturation of the circuit implementation. It can be varied between *0.25* V and *1.0* V.

C. *Synthesis of the Sinusoidal Wave Signals*

As it is shown in Fig. 4, the outputs of the triangle wave oscillators drive the corresponding low distortion triangle-sine wave converter circuit which is analyzed in [13], [14] and [15]. The relation between the base-emitter voltage v_{be} and the collector current I_c is given as,

$$I_c \approx I_s \exp\left(\frac{Q}{kT} v_{be}\right) \tag{13}$$

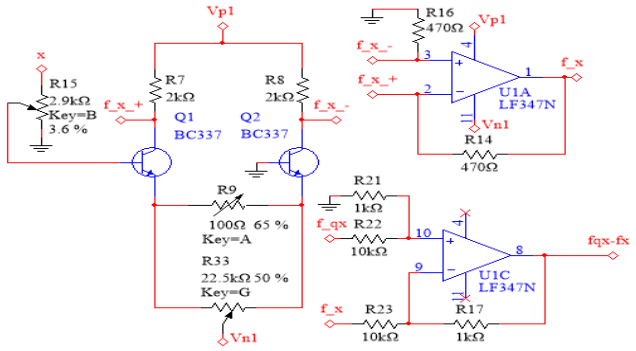

Fig. 4. The triangle-sine wave converter, the synthesis of the signals f(x), and f(qx)—f(x).

where I_s is the saturation current, Q is the electron charge, k is the Boltzmann's constant and T is the absolute temperature. One of the triangle-sine wave converters together with the current to voltage converter to obtain the corresponding sinusoidal waveform f(x) is shown on the left and on the top right of Fig. 4, respectively. The differential amplifier topology used to synthesize the difference signal f(qx)—f(x) is shown at the bottom right of Fig. 4. The signal f(qx)—f(x) that has been used on the numerator of the q-derivative operation represents the change in f(x) due to the scale change in its independent variable x. The signal f(qx) has been synthesized using another triangle-sine wave converter and current to voltage converter combination not shown in Fig. 4, due to the page limitation. The q-derivative of an arbitrary function can be realized if only the triangle-sinusoidal wave converters are replaced with generators i.e. an arbitrary function generator or any other designed synthesizer circuit capable of generating the desired analog waveform of interest. Technical information for BC337 and LF347 can be found in [16] and [17] respectively.

D. *Synthesis of the Analog q-derivative Signal*

The analog division operation is done using AD633 four quadrant analog multiplier [18] as seen in Fig. 5. The analog division operation is accomplished by using AD633 in the feedback loop of the LF347 opamp. The transfer function of AD633 is given in (13). Referring to the signal and the circuit element labels in Fig. 5, and setting $X_2 = 0$, $Y_2 = 0$, $Z = 0$, the transfer function for the division is derived as,

$$W = \frac{(X_1 - X_2)(Y_1 - Y_2)}{10} + Z \tag{14}$$

$$W = -\frac{R_{35}}{R_{28}}\left(\mathrm{f}(qx) - \mathrm{f}(x)\right) \tag{15}$$

$$W = \frac{X_1 Y_1}{10} = \frac{\left(q\,\mathrm{tri}(x) - \mathrm{tri}(x)\right)\left(\mathrm{f}_{\mathrm{q\_deriv}}(x)\right)}{10} \tag{16}$$

And finally, the output of our proposed circuit (q-derivative) has been obtained as,

$$\mathrm{f}_{\mathrm{q\_deriv}}(x) = -10\frac{R_{35}}{R_{28}}\frac{\left(\mathrm{f}(qx) - \mathrm{f}(x)\right)}{\left(q\,\mathrm{tri}(x) - \mathrm{tri}(x)\right)}. \tag{17}$$

The ratio of R_{35} / R_{28} in (17) can be used to cancel the multiplier 10. The simulation results are given as in Fig. 6, Fig. 7, and Fig. 8.

Remark: We have also verified our implementation by applying the q-periodic Weierstrass function $\mathrm{f_W}(x)$ at the input of the analog q-differentiator and observing zero function at the output consistent with $\mathrm{D_q f_W}(x) = 0$ where the q-Weierstrass function $\mathrm{f_W}(x)$ is given in [3] and [8] as

$$\mathrm{f_w}(x) = \sin\left(\frac{2\pi}{\ln q}\ln x\right). \tag{18}$$

[1] The syntactic differences between the mathematical formulas and the signal naming in the schematics seen in this paper are due to the signal naming convention of the SPICE program e.g. underscore character is used in the schematics instead of parenthesis character.

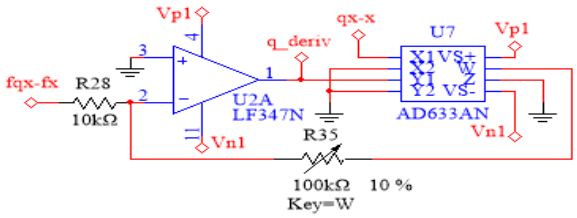

Fig. 5. The analog division circuit for implementing q-derivative operator.

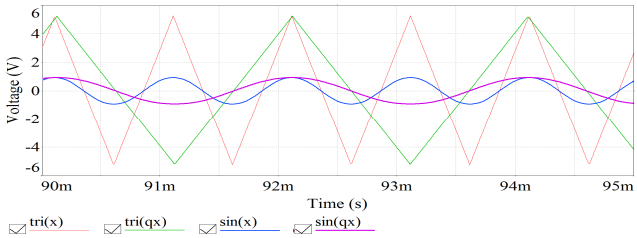

Fig. 6. Synthesized signals *tri(x)*, *tri(qx)*, *sin(x)* and *sin(qx)*.

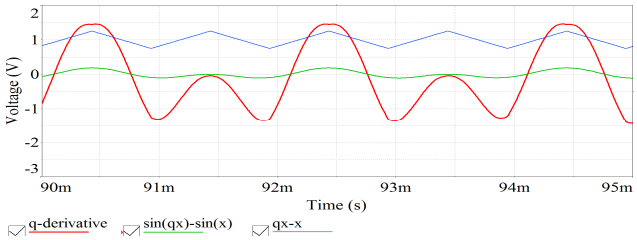

Fig. 7. Synthesized signals $f_{q\ deriv}(x)$, $\sin(qx)$— $\sin(x)$, $q\text{tri}(x)$ —$\text{tri}(x)$.

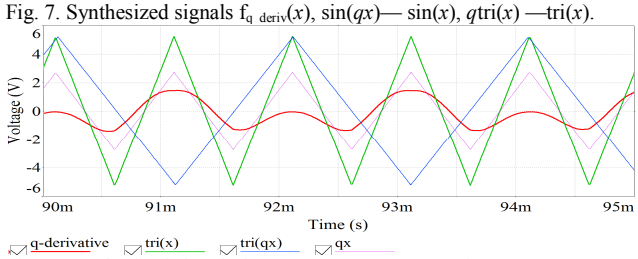

Fig. 8. Synthesized signals $f_{q\_deriv}(x)$, *tri(x)*, *tri(qx)*, $q\text{tri}(x)$.

Q-Derivative Circuit Hardware Implementation

Our test setup consist of Tektronix AFG3102 Arbitrary Function Generator, Tektronix TDS2202C Oscilloscope, a symmetric DC power supply for $V_p = 12$V, $V_n = -12$V and Mastech 30V, 3A DC power supply for additional offset voltage V_r. As mentioned in section III, the operation frequencies for the oscillators are $f_1 = 2$ Hz, $f_2 = qf_1 = 1$ Hz where the scaling parameter q is selected as $q = 0.5$. The oscilloscope traces for the realized analog q-derivative hardware is shown in Fig. 9. The output of the q-derivative for one period of the oscillator output are consistent with the analytical results. However, noise inevitably affects the output of the real devices compared to their models implemented in simulation. Therefore, the output of the materially realized q-derivative circuit is observed as the sum of the circuit noise and the q-derivative signal. However, low tolerance passive elements, low noise precision operational amplifiers and the implementation of the printed circuit board design techniques to enhance the electromagnetic compatibility will reduce the inevitable circuit noise to the minimum.

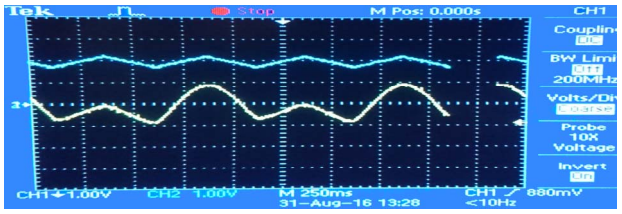

Fig. 9. The real-time oscilloscope traces of the implemented analog q-derivative hardware. The upper trace is the $q\text{tri}(x)$—$\text{tri}(x)$ signal for given Vr. The lower trace is $Dqf(x)$ where $f(x) = \sin(x)$.

Conclusion and Future Work

The hardware implementation of q-derivative circuit and its SPICE simulation are seen to be consistent with the theoretical results. Our future works include the analog realization of Jackson's q-integral operator and the implementation of the q-oscillator circuit to observe q-periodic Weierstrass function. One of our other future works is to realize a q-Weierstrass synthesizer to verify our proposed q-derivative circuit hardware realization which would yield a zero function at its output with such a synthesized q-Weierstrass function at its input.

References

[1] V. Kac, and P. Cheung, Quantum Calculus. New York: Springer, 2002.

[2] T. Ernst, Treatment of Q-Calculus. Uppsala: Birkhauser, 2012.

[3] T. Ernst, The history of q-calculus and a new method, Uppsala, 2000.

[4] F. H. Jackson, A basic sine and cosine with symbolic solutions of certain differential equations, Proc. Edin. Math. Soc. 22, pp. 28-39, 1904.

[5] M. F. Barnsley, Fractals Everywhere, 2nd ed., Cambridge, MA: Academic Press, Inc., 1993.

[6] S. Erkus, Q-periodicity self-similarity and Weierstrass-Mandelbrot function, MSc thesis, Izmir Institute of Technology, Izmir, 2013.

[7] M. Bohner, and A. Peterson, Dynamic Equations on Time Scales, an introduction with applications, New York, NY: Birkhauser, 2001.

[8] S. Nalci, and O. Pashaev, Q-damped oscillator and degenerate roots of constant coefficients q-difference ODE, arXiv:1107.2518 [math.CA], 2013.

[9] S. Nalci, and O. Pashaev, Q-analog of shock soliton solution, J. Phys. A: Math. Theor. 43, 445205, 2010.

[10] A. Erzan, Q-calculus and irreversible dynamics on a hierarchical lattice, Tr. J. of Physics, vol. 23, pp. 9-19, 1999.

[11] P. Horowitz, W. Hill, The Art of Electronics, 3rd ed., New York, NY: Cambridge University Press, pp. 239, 2015.

[12] S. Franco, Design with Operational Amplifiers and Analog Integrated Circuits, 4th ed., New York, NY: McGraw Hill, pp. 505-507, 2015.

[13] R. G. Meyer, W. M. C. Sansen, S. Liu, and S. Peeters, The differential pair as a triangle-sine wave converter, IEEE Journal of Solid-State Circuits, vol. 11, issue 3, pp. 418-420, June 1976.

[14] W. A. Evans, V. Schiffer, A low distortion tri-wave to sine converter, The Radio and Electronic Engineer, vol. 47, no. 5, pp. 217-224, May 1977.

[15] N. Ozkurt, F. A. Savaci, and M. Gunduzalp, The circuit implementation of a wavelet function approximator, Analog Integrated Circuits and Signal Processing, 32, Kluwer Academic Publishers, pp. 171-175, 2002.

[16] Fairchild, BC337/BC338 NPN epitaxial silican transistor datasheet, September, 2015.

[17] Texas Instruments, LF147/LF347 wide bandwidth quad JFET input operational amplifiers datasheet, March 2015.

[18] Analog Devices, A low cost analog multiplier AD633 datasheet, March 2015.